Condensation out of Steam-Air-Mixtures in a Horizontal Annular-Flow-Channel

G. Nolte and F. Mayinger

TECHNISCHE UNIVERSITÄT MÜNCHEN
LEHRSTUHL A FÜR THERMODYNAMIK
o. PROF. DR.-ING. F. MAYINGER
Arcisstr. 21, 8000 München 2
Tel.: (089) 2105-3450 Telex: 522854 TUM

Abstract

Experiments were performed on the condensation of steam out of steam-air-mixtures in annular flow at the inner tube cooled. The range of investigations was varied at laminar and turbulent flow between $1.5 \cdot 10^3 \leq Re \leq 1.3 \cdot 10^4$ and the inlet concentration between $0.59 \leq p_{steam}/p_{total} \leq 0.95$. The measurements, performed at an open test loop at $p_{total} \approx 0.96$ bar, allowed to evaluate the local heat and mass transfer coefficient for various inlet lengths in the $2m$ long annulus.

The change in heat and mass transfer is mainly influenced by the increasing air fraction and the decreasing mass flow rate along the tube. Due to the convective mass transport and the condensation of steam at the surface of the water-film gradients of steam concentration and of temperature occur axially and radially in the flow channel.

The steam concentration was locally measured inside the annulus with a newly developed dew point probe. The concentration measurement is based on the determination of the dew point temperature and the total pressure of the gas mixture, from which the concentration of the condensing component in the gas mixture can be calculated by simple rules of thermodynamics. Especially in circumferential direction an increase of the air fraction at the bottom of the tube along the flow path could be observed.

The heat flux was locally measured by using the temperature gradient in the cooled inner tube. Its variation in circumferential direction is a function of the thickness of the liquid film as well as of the turbulence in this film.

The experiments showed near the inlet region a slightly higher heat flux at the bottom of the tube compared to the top although it should be smaller there due to a thicker liquid film. Far downstream from the inlet region the heat transfer at the top was higher than at the bottom.

The reasons for the above mentioned effects will be discussed in this paper yielding a better understanding of the thermal and fluid processes involved in condensation out of vapor-gas- mixtures. The measured data allow to develop correlations for predicting the local Nusselt and Sherwood numbers in a horizontal annular-flow-channel.

1.) Introduction

In a great number of technical apparatus, i.e. in the chemical and energy industry, the process of condensation in the presence of uncondensables is encountered. For example in heat exchangers already little amount of an uncondensable gas has strong influence on the transfered energy flow.

Published 1988 by Elsevier Science Publishing Co., Inc.
Experimental Heat Transfer, Fluid Mechanics, and Thermodynamics 1988
R.K. Shah, E.N. Ganić, and K.T. Yang, Editors

Experimental investigations on the partial condensation are not very numerous. Marschall /1/ and Lehr /2/ were describing the heat and mass transfer from binary mixtures at the inner side of a cooled vertical tube. Ackermann /3/ investigated the condensation out of steam-air mixtures inside a single vertical tube. The condensation of different vapors in the presence of air was researched by Gerhart /4/ in a vertical mounted annulus, with the inner tube cooled. Dallmeyer /5/ investigated the partial condensation with special effort to the laminar and turbulent boundary layers at a vertical flat plate at longitudinal flow.

The above mentioned experimental studies were carried out at different test sections but all vertically mounted with a vertical flow direction.

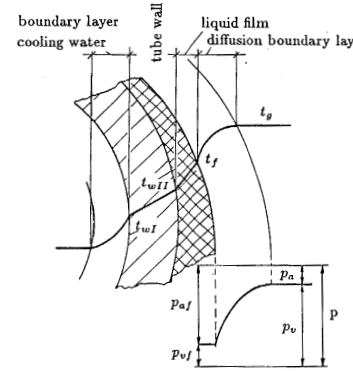

Fig. 1: *Temperature and partial pressure curve at partial condensation*

In this work the mechanism of heat and mass transfer along a cooled horizontal tube with the condensation of steam out of a steam-air mixture in an annular-flow-channel is investigated. The heat and mass transfer is mainly influenced by the condensing film flowing around the inner cooled tube and an increasing air fraction from the bulk of the annulus (partial pressure p_a) to the film-surface (p_{af}). In contrast to pure steam condensation the steam is transfered by convection and diffusion and also a temperature profile (t_g-t_f) in the gas phase can be observed (see Fig. 1). First results on the condensation of steam out of steam-air-mixtures at laminar and turbulent annular flow with varying inlet concentrations will be presented in this paper.

2.) Description of the experimental setup

The measurements of condensation in the presence of an inert gas were performed at an open test loop consisting of the following main equipment as demonstrated in Fig. 2: the electrical heated boiler producing the steam, the pressurized air tank, the air heater, the heat exchanger including the measuring section and a cooling water supply.

The steam and the air flow rates are measured separately in calibrated orifice flow meters. The air is passing an electrical heater before mixed with the steam and enters then the heat exchanger. To avoid condensation on the way to the test section the steam is superheated according its higher pressure in the boiler.

The heat exchanger consists of two concentric tubes. The inner tube is cooled with water, the outer tube insulated. In the annulus between the outer and inner tube (hydraulic diameter d_h=2s=15.5·10^{-3}m) the condensing gas mixture flows.

To enable local measurements of heat and mass transfer along the heat exchanger tube with a condensing length of 2m, an instrumented section with a length of 0.25m was installed and the gas inlet was constructed movable in axial direction. This was achieved by a pipe consisting of two concentric tubes which was stuck movable into the gas annulus.

As shown in Fig.2, the steam-air-mixture is passing through the pipe insulated by an air space from the water cooled tube to avoid condensation on its way through before entering the condensing flow path. The distance between the onset of condensation and the inlet of the measuring section could be varied by this device from 0 up to 1.75m in 0.25m steps in order to get eight measuring intervals at a total length of 2m.

The test section

The test section, illustrated in Fig. 3, has a condensing length of 0.25m and is part of the heat exchanger described above. The temperature difference of the gas mixture from the inlet "1" to the outlet "2" is measured with two thermocouples (t_{g1}, t_{g2}).

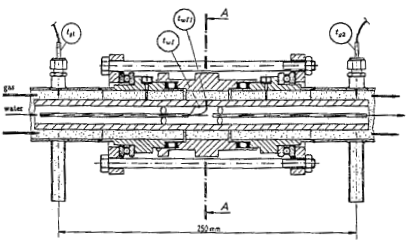

Fig. 3: *Test section*

The wall heat flux through the watercooled stainless steel

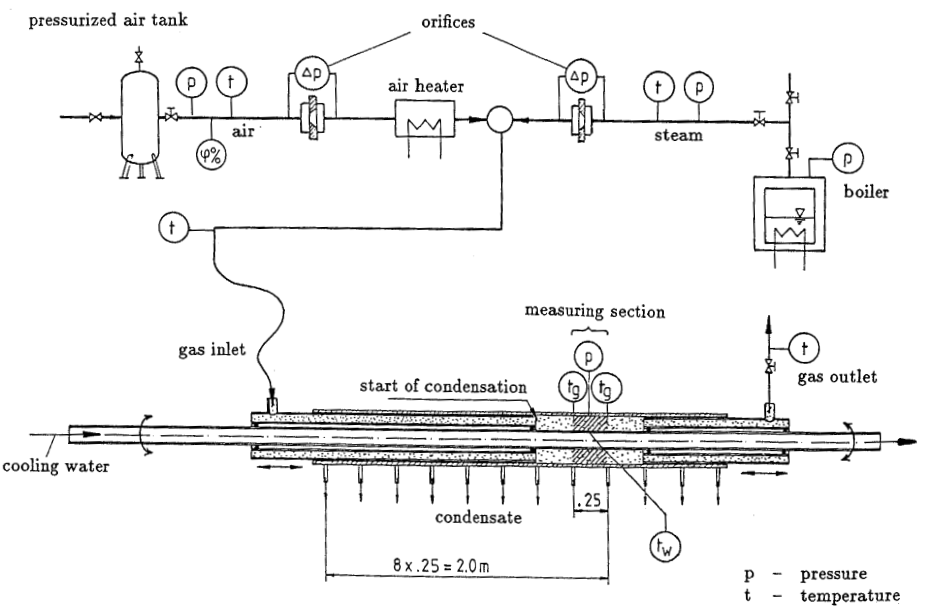

Fig. 2: *Experimental setup*

tube (ϕ0.025m×0.005m) can be calculated from the wall temperatures of the tube. Four thermocouples ($0.5{\cdot}10^{-3}m$ in diameter) are soldered in the wall – two at the outer (t_{wo}) and two at the inner surface (t_{wi}) of the tube. In order to get the circumferential temperature distribution the tube can be turned. Fig. 4 shows a cut through the middle of the measuring section where the cooled inner tube surrounded by a turnable ring can be seen. In this ring two measuring divices are installed:

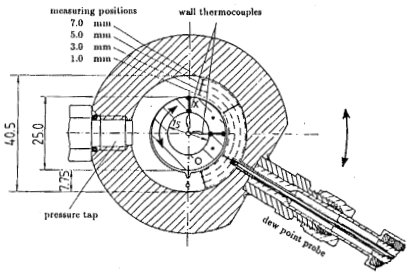

Fig. 4: *Cut A-A through the middle of the measuring section*

1) a pressure tap, measuring the total pressure p,
2) a dew point probe for the determination of the steam-air fraction in radial and circumferential direction.

3.) Measuring technique

Dew point probe

The aim of the newly developed dew point probe is to obtain the local concentration of non-condensables in a condensing atmosphere. The measurement is based on the determination of the dew point temperature t' and the total pressure p of the gas mixture.

Assuming the validity of the ideal gas law we can calculate the mass ratio m_{nc}/m_c of the non-condensing (m_{nc}, here: air) and the condensing gas (m_c, here: steam)

$$\frac{m_{nc}}{m_c} = \frac{p - p_c}{p_c} \cdot \frac{R_c}{R_{nc}} = \frac{1 - \psi_c}{\psi_c} \cdot \frac{R_c}{R_{nc}} \qquad (1)$$

with R_c and R_{nc} as the specific gas constants and ψ_c as the pressure ratio of the partial pressure p_c of the condensing gas to the total pressure p:

$$\psi_c = \frac{p_c}{p} \qquad (2)$$

As the total pressure p does not exceed $\sim$ 10bar and the presence of the non-condensing gas has negligible influence on the saturation partial pressure p_c', the unknown partial pressure p_c can be assumed equal to the saturation pressure p_c' at the dew point temperature t' of the gas mixture. That is to say

$$p_c = f(t') \qquad (3)$$

The dew point temperature t' can be measured with the probe shown in Fig. 5.

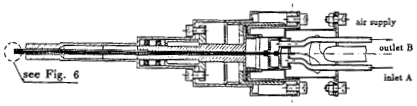

Fig. 5: *Dew point probe*

The measuring sensor is a device consisting of a miniature thermocouple soldered to a $\sim 0.1{\cdot}10^{-3}m$ thin copper foil that separates the steam atmosphere from an inner channel system (see Fig. 6), through which the copper foil can be cooled with air from the rear side.

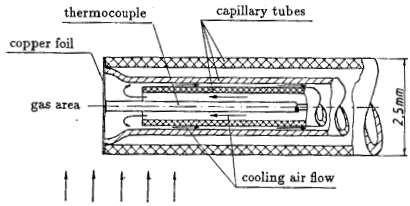

Fig. 6: *Top of the dew point probe*

The inner capillary tubes of the channel system are connected to an air supply with an inlet A and an outlet B. The two outer capillary tubes form an insulating space to avoid condensation at the outer tube wall of the probe.

As soon as starting the air cooling the temperature at the copper foil falls. Fig. 7 shows three typical temperature curves recorded with a continuous line recorder. Curve 1 was detected in a pure steam flow, curve 3 in a pure air flow and curve 2 was detected in a mixture of steam and air.

Curve 2 shows – after the start of cooling – a smooth decrease in the temperature until condensation at the outside of the copperfoil starts and a sudden strong change in the gradient can be observed. This marks the dew point temperature from which the steam concentration of the investigated gas mixture can be calculated.

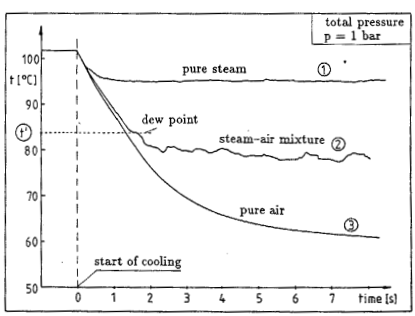

Fig. 7: *Temperature curve at the top of the dew point probe in (1) pure steam, (2) a steam-air mixture and (3) pure air*

The scattering of the temperatures read out from the strip charts at the points of strong gradient change lies within $\pm$ 0.25K resulting in uncertainties for ψ ranges i.e. from $\Delta\psi \approx \pm 0.01$ (for $\psi = 0.95$) to $\Delta\psi \approx \pm 0.002$ (for $\psi = 0.1$).

4.) Evaluation

The varying heat and mass transfer in axial direction is mainly influenced by a decreasing steam flow rate

$$\dot{M}_{v2} = \dot{M}_{v1} - \mid \dot{M}_{cond} \mid \tag{4}$$

and a constant air flow rate,

$$\dot{M}_{a2} = \dot{M}_{a1} = const. \tag{5}$$

further a temperature and air fraction profile in the radial direction in the gas phase.

The total heat transfer from the gas to the cooled wall is controlled by three heat transporting phenomena:

1.) $\dot{Q}_m$ due to the phase change of the condensing steam at the film surface,

2.) $\dot{Q}_d$ due to the convection in the gas annulus,

3.) $\dot{Q}_c$ due to the convective transport in the liquid film.

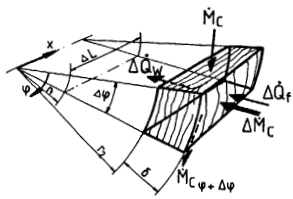

Fig. 8: *Reference volume at the liquid film*

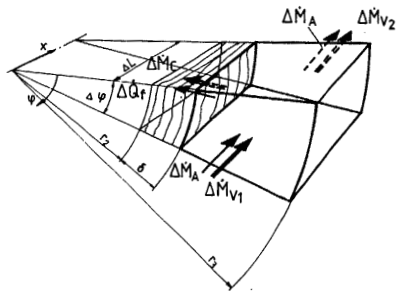

Fig. 9: *Reference volume at the gas annulus*

Neglecting the axial heat transfer in the cooled tube, the total heat flux $\dot{Q}_w$ can be expressed by

$$\dot{Q}_w = \dot{Q}_m + \dot{Q}_d + \dot{Q}_c \ . \tag{6}$$

Combining the energy balance at the liquid film (see Fig. 8)

$$\Delta\dot{Q}_w = \dot{M}_c \cdot h_c - \left(\dot{M}_c + \frac{d\dot{M}_c}{d\varphi}\Delta\varphi\right) \cdot h_{c|_{\varphi+\Delta\varphi}} + \Delta\dot{Q}_f \tag{7}$$

with the energy balance in the gas annulus (see Fig. 9)

$$\Delta\dot{Q}_f = \Delta\dot{M}_a \cdot h_{a1} - \Delta\dot{M}_a \cdot h_{a2} + \Delta\dot{M}_{v1} \cdot h_{v1} - \Delta\dot{M}_{v2} \cdot h_{v2} - \Delta\dot{M}_c \cdot \Delta h_v[t_f] \tag{8}$$

the total heat flux $\tilde{\dot{Q}}_w$ averaged over the length of the measuring section becomes

$$\left.\begin{aligned} \tilde{\dot{Q}}_w = {} & \widetilde{\dot{M}}_{cond} \cdot \Delta h_v[\tilde{t}_f] \\ & -\left(\dot{M}_a \cdot c_{pa} + \widetilde{\dot{M}}_v \cdot c_{pv}\right) \cdot (t_{g1} - t_{g2}) \\ & +\widetilde{\dot{M}}_{cond} \cdot c_{pv} \cdot (\tilde{t}_g - \tilde{t}_f) \\ & -\widetilde{\dot{M}}_{cond} \cdot c_c \cdot (\tilde{t}_f - \tilde{t}_{cond}) \end{aligned}\right\} \begin{aligned} & \tilde{\dot{Q}}_m \\ & \tilde{\dot{Q}}_d \\ & \tilde{\dot{Q}}_c \end{aligned} \tag{9}$$

In Eq. (9) the wall heat flux $\tilde{\dot{Q}}_w$, the condensate flux $\widetilde{\dot{M}}_{cond}$ the temperature $\tilde{t}_f$ at the film surface and the temperature $\tilde{t}_{cond}$ of the dropping film at the bottom of the tube are unknown.

The wall heat flux $\tilde{\dot{Q}}_w$ can be calculated from the measured wall temperatues t_{wi} and t_{wo} to

$$\tilde{\dot{Q}}_w = \frac{\lambda_w}{r_2 \cdot ln\frac{r_2}{r_1}} \cdot 2\pi r_2 \cdot \Delta L \cdot (\tilde{t}_{wi} - \tilde{t}_{wo}) \tag{10}$$

In contrast to the "Nusseltsche Wasserhauttheorie" the film surface temperature t_f cannot be assumed to be constant and also the influence of the condensate subcooling ($t_f - t_{cond}$)cannot be neglected. It can be calculated from the energy-balance at the laminar film (see Fig. 10)

$$\frac{\partial\dot{H}}{\partial\varphi} \cdot \Delta\varphi + \frac{\partial\dot{Q}}{\partial r} \cdot \Delta r = 0 \tag{11}$$

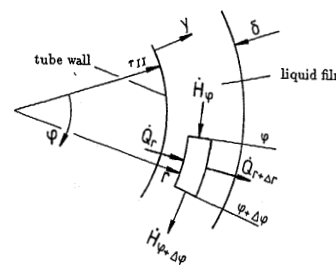

Fig. 10: *Energy balance in the liquid film*

combined with the momentum balance yielding the differential equation

$$\frac{\partial}{\partial\varphi}\left(\frac{\rho_c^2\cdot g\cdot\sin\varphi}{\eta_c}\cdot\left(\delta_\varphi\cdot y-\frac{y^2}{2}\right)\cdot c_c\cdot t\right)+\frac{\partial}{\partial r}\left(\lambda_c\cdot r\frac{\partial t}{\partial r}\right)=0 \tag{12}$$

which was solved numerically. The film-thickness δ_φ can be calculated from

$$\delta_\varphi=\sqrt[3]{\frac{\dot{M}_c(\varphi)\cdot 3\cdot\eta_c}{\rho_c^2\cdot g\cdot\sin\varphi\cdot\Delta L}} \tag{13}$$

Definition of the Nusselt- and Sherwood-Number

The resistance for the transport of the "dry" heat flux $\dot{Q}_d$ from the bulk of the gas flow to the film surface can be described by the so-called "dry heat transfer coefficient" α_d according to

$$\tilde{\dot{Q}}_d=\alpha_d\cdot 2\pi r_2\cdot\Delta L\cdot(\tilde{t}_g-\tilde{t}_f) \tag{14}$$

The resistance to the heat flux $\dot{Q}_m$ is described by the mass transfer coefficient β according to

$$\tilde{\dot{Q}}_m=\beta\cdot\frac{p}{R_v}\left[\left(\frac{\tilde{\psi}_v}{T_v}\right)_g-\left(\frac{\tilde{\psi}_v}{T_v}\right)_f\right]\cdot 2\pi r_2\cdot\Delta L \tag{15}$$

The heat transfer is characterized by the Nusselt (Nu) number, defined by

$$Nu=\frac{\alpha_d\cdot 2s}{\lambda_g} \tag{16}$$

and the mass transfer by the Sherwood (Sh) number

$$Sh=\frac{\beta\cdot 2s}{D}\ . \tag{17}$$

5.) Experimental results

The results of three arbitrary selected experimental runs are presented. The inlet conditions can be characterized by the Re number

$$Re=\frac{w_g\cdot 2s}{\nu_g}, \tag{18}$$

the steam-air fraction $\psi_{in}=p_{steam}/p_{total}$, the temperature t_g of the gas mixture and the total pressure p. The varying parameter in these runs was the pressure ratio ψ_{in} at the inlet as a measure for the steam fraction ranged from 0.55 to 0.95 as can be seen in Table 1:

Table 1: Inlet conditions of the steam-air mixtures

	ψ_{in}	Re_{in}	t_{gin}[°C]	p[bar]
run 1	0.95	$7.9\cdot 10^3$	104	0.96
run 2	0.78	$7.9\cdot 10^3$	104	0.96
run 3	0.59	$7.9\cdot 10^3$	104	0.96

In Fig. 11 the Re number is plotted versus the condensing length l. Due to the condensation of the steam all three runs show a decrease in the Re number. The higher decrease of the Re number in run 1 compared to run 2 and run 3 can be explained by a lower air mass flow rate due to the different concentrations ψ_{in} at the inlet. The corresponding gas velocities are ranging i.e. for run 1 from 11.0 m/s at the inlet to 0.65 m/s at the outlet.

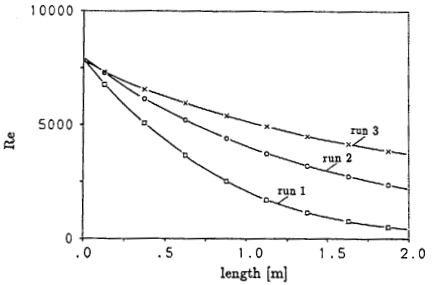

Fig. 11: *Re number ($d_h = 2s$) versus the tube length*

The next figures, Fig 12 a and b, show the temperature curve from the inner water cooled tube wall through the waterfilm to the bulk of the gas mixture. The radial data were taken at three different axial positions, namely 0.125m, 0.875m and 1.875m from the inlet of the annulus. The temperature t_g of the gas mixture and the wall temperatures t_{Wi}, t_{Wo} were measured. The temperature t_f at the film surface was calculated from the energy and momentum balance in the film, Eqs. (11) and (12).

The temperature difference $(t_g - t_f)$ between the gas mixture and the film surface is used when defining the convective "dry" heat transfer coefficient. From the temperature gradient in the material of the tube wall the total heat flux can be calculated.

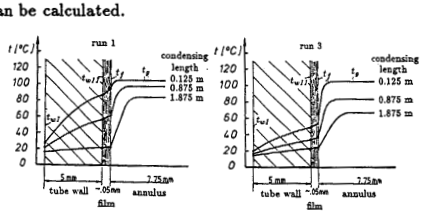

Fig. 12a,b: *Temperature curve from the inner watercooled tube to the gas annulus*

In Fig. 13 the heat flux density averaged over the circumference of the tube is plotted versus the tube length. After a flow path of approximately 1.5m most of the steam in the gas mixture has been condensed and the curves of the three different inlet steam concentrations tend to fall together.

An impression of the mean steam concentration in the annulus and at the surface of the liquid film can be derived from Fig. 14. It shows the pressure ratio ψ_m averaged over the circumference of the annulus versus the condensing length. The pressure ratio at the film surface (dotted line) was evaluated from the calculated temperature at the

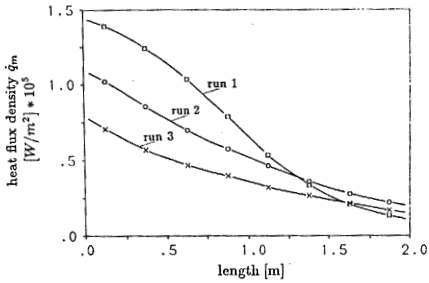

Fig. 13: *Mean total heat flux density $\dot{q}_m$*

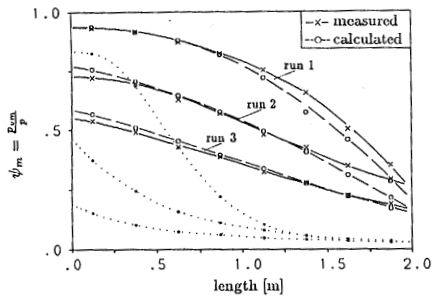

Fig. 14: *Pressure ratio $\psi_m = p_{vmean}/p_{total}$ in the gas annulus (—) and at the film surface (···)*

film surface derived from Eqs. (11) and (12) assuming saturated vapor $\psi_f = p'_{steam}[t_f]/p$. The mean pressure ratio in the gas annulus was calculated from the energy and mass balance and also measured with the dew point probe. The measured and calculated curves show very good agreement. The deviation can be explained by an error less than 2% in the measurement of the steam or air flow, respectively.

In order to describe the mass transfer to the cooled tube the concentration profile had been determined with the dew point probe in radial, circumferential and longitudinal direction inside the annular flow channel. The measured data selected at three axial positions (0.125m, 0.875m, 1.875m from the inlet of the annulus) are demonstrated in Fig. 15 a,b,c, where $y = 0mm$ locates the film surface.

As to be expected the condensation at the cooled tube yields an increase in the concentration profile in radial and a decrease in axial direction. An interesting effect can be observed in the profiles at circumferential direction. An idea how this profile looks like can be derived by comparing at one and the same axial and radial position the concentration at the top of the annulus (15°) and at the bottom (165°).

At the inlet of the annulus the concentration profile is balanced over the circumference. With increasing condensing length a higher concentration at the top compared to

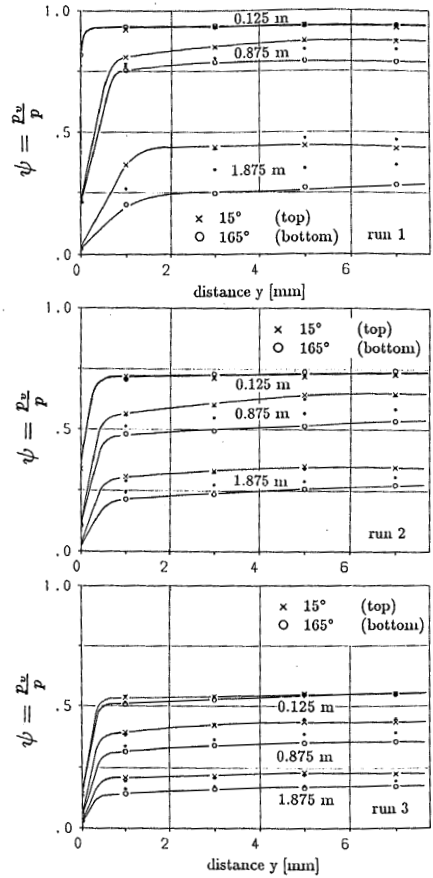

Fig. 15a,b,c: *Pressure ratio $\psi = p_{steam}/p_{total}$ versus the distance of the film at three axial positions of the condensing length*

the bottom can be observed. Far downstream, when the steam-air flow is developing into a pure air flow with a little amount of saturated steam, the radial profile at the top and at the bottom tend to fall together as can be seen in Fig. 15 c, comparing the radial profiles at the end (1.875m) and in the middle (0.875m) of the annulus.

The local heat flux has been evaluated from the temperature gradient in the material of the cooled tube, which was determined with two thermocouples positioned near the inner and outer side of the tube. In order to measure the heat flux profile over the circumference the tube was installed turnable. It is, as to be expected, depending on the thickness of the liquid film flowing around the cooled tube and of the turbulence in this film.

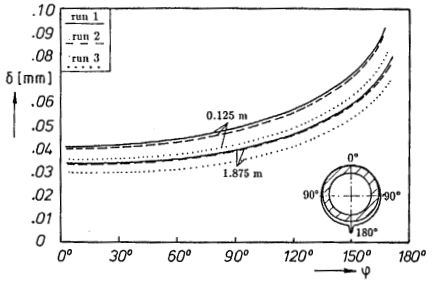

Fig. 16: *Calculated film thickness in circumferential direction at the inlet (0.125m) and the outlet (1.875m) of the annulus*

The thickness of the liquid film was calculated from Eq. (13) over the circumference of the tube and varied between $0.03\text{-}0.05 \cdot 10^{-3} m$ at the top up to $0.1 \cdot 10^{-3} m$ at the bottom as shown for run 1,2 and 3 in Fig. 16 for two axial positions at the inlet and outlet of the tube. It should be noticed that in this calculation the influence of the axial shear stress at the gas liquid interface is not yet included.

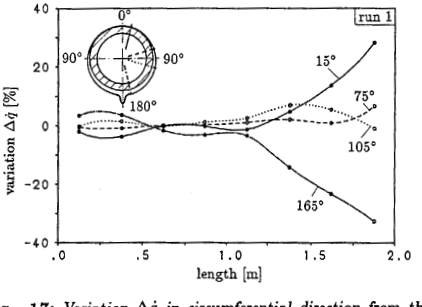

Fig. 17: *Variation $\Delta\dot{q}$ in circumferential direction from the mean heat flux*

Fig 17. shows the variation of the heat flux in circumferential direction compared to the mean heat flux locally averaged over the surface of the tube. Due to a higher thickness of the liquid film at the bottom of the tube the heat flux should be smaller there. The experiments, however, showed near the inlet region a slightly higher heat flux at the bottom compared to the top. This tendency occured at all three runs and is demonstrated for run 1 in Fig. 17. Due to the liquid separation at the bottom of the tube wall a higher turbulence can be observed especially at the inlet region, where the flow turbulence and in particular the condensing mass flow rate is higher.

Far downstream from the inlet region the heat transfer at the top was higher than at the bottom. Along the flow path the gas velocity and also the condensing mass flow are decreasing, which reduces the momentum and shear transfer between the gas and the liquid film yielding a lower

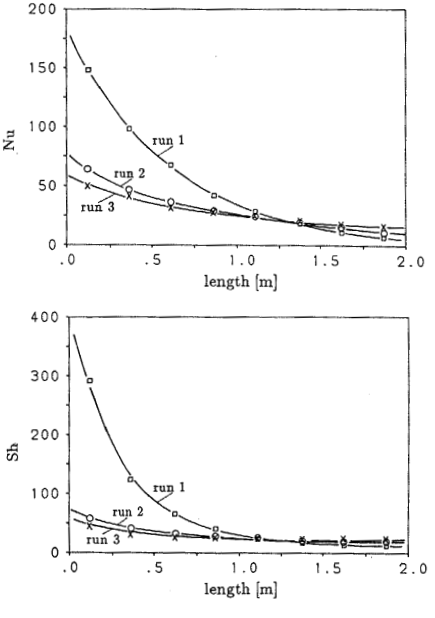

Fig. 18a,b: *Nu and Sh number (mean values over the circumference) versus the tube length*

turbulence in the film and also in the gas flow. Beside that, the dew point measurements showed in axial direction a balanced profile over the circumference at the inlet of the annulus. Downstream the concentration of air at the bottom was rising more than at the top which yielded an additional resistance for the heat and mass transfer at the bottom of the tube.

Finally, the local Nusselt- and Sherwood numbers describing the heat and mass transfer from the gas to the liquid film were calculated from the measured temperature and steam-air fraction according to Eqs. (14)-(17). The local mean values averaged over the circumference of the tube are plotted in Fig. 18 versus the tube length and in Fig. 19 versus the local Re number.

Due to the higher turbulence and a higher condensing rate at the inlet the curves show the typical developing flow from the inlet downstream the condensing length. At the inlet the Nu and Sh numbers are rising from run 3 to run 1 with increasing steam fraction. Far downstream most of the steam has been condensed and the heat and mass transfer is mainly influenced by the air mass flow so that the curves in Fig. 18 tend to fall together. The air mass flow, which is assumed to be constant over the tube length, is decreasing with increasing pressure ratio ψ_{in} from run 1 over run 2 to run 3. Due to a lower air mass flow run 1 shows slightly lower Nu and Sh numbers at the end of the tube compared to run 2 and run 3.

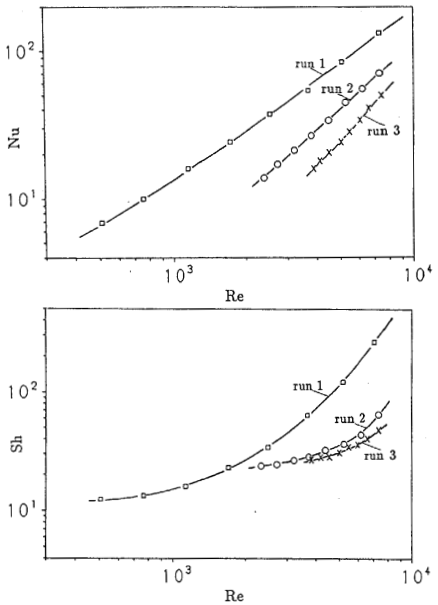

Fig. 19a,b: *Nu and Sh number (mean values over the circumference) versus the Re number*

Analyzing the curves of the local Nu and Sh numbers versus the Re number in Fig. 19 we find a strong decrease in the Re number and in the heat and mass transfer due to the decreasing steam flow and decreasing gas velocity along the flow path.

6.) Conclusions

Experiments on the condensation of steam out of steam-air-mixtures in turbulent and laminar flow have been carried out in a horizontal annular-flow-channel. Temperature and concentration measurements were performed in radial, circumferential and longitudinal direction at a 2m long test section with varying inlet concentrations. The heat and mass transfer was described by the local Nusselt and Sherwood numbers versus the Reynolds number or versus the condensing length of the tube, respectively. The work for the future will be to develop correlations for predecting the Nusselt and Sherwood numbers for different steam- air fractions and varying Re numbers.

Nomenclature

c	$[J/kgK]$	specific heat capacity
d_h	$[m]$	hydraulic diameter
D	$[m^2/s]$	binary diffusion coefficient
$\dot{H}$	$[J/s]$	enthalphy flow
h	$[J/kgK]$	specific enthalphy
Δh_v	$[J/kgK]$	latent heat of condensation
Δl	$[m]$	length of the measuring section
m	$[kg]$	mass
$\dot{M}$	$[kg/s]$	mass flow
Nu	-	Nu number
p, p_{total}	$[N/m^2]$	total pressure
p_a	$[N/m^2]$	air pressure
p_v	$[N/m^2]$	vapor pressure
$\dot{Q}$	$[W]$	heat flux
$\dot{q}$	$[W/m^2]$	heat flux density
w	$[m/s]$	velocity
R	$[J/kgK]$	spec. ideal gas constant
r	$[m]$	radius
Re	-	Re number
s	-	width of the annulus
Sh	-	Sherwood number
t_{cond}	$[°C]$	condensate temperature
t_f	$[°C]$	film surface temperature
t_g	$[°C]$	bulk temperature in the gas annulus
t_w	$[°C]$	wall temperature
y	$[m]$	wall distance
δ_φ	$[m]$	condensate film thickness
λ	$[W/mK]$	thermal conductivity
φ	$[°]$	angle in circumferential directon
η	$[kg/ms]$	dynamic viscosity
ν	$[m^2/s]$	kinematic viscosity
ρ	$[kg/m^3]$	density
ψ	-	pressure ratio (p_{steam}/p_{total})

Subscripts

$\sim$	mean value
'	saturated
1,2	inlet, outlet of the measuring section
I,II	innerside, outerside of the cooled tube
a	air
c,nc	condensable, non condensable gas
f	at the film surface
g	in the gas annulus
i,o	at the inner/outer side
in	at the inlet
v	vapor
w	at the tube wall

References

/1/ **Marschall, E.** *Wärmeübertragung bei der Kondensation von Dämpfen aus Gemischen mit Gasen.* Abh. Dtsch. Kältetechnischer Verein Nr. 19 Karlsruhe: C.F. Müller 1967.

/2/ **Lehr, G.** *Wärme- und Stoffübertragung bei der Kondensation von zwei Dämpfen aus einem Gemisch mit einem Inertgas.* Diss. an der TU Hannover 1972.

/3/ **Ackermann, D.** *Wärme- und Stoffübertragung bei der Kondensation eines Dampfes aus einem Gemisch mit einem nicht kondensierbaren Gas in laminarer und turbulenter Strömungsgrenzschicht.* Diss. an der Universität Stuttgart 1972.

/4/ **Gerhart, K.** *Stoff- und Wärmeübertragung bei der Kondensation von Dämpfen aus im Ringspalt strömenden Gemischen mit Luft.* Diss. an der TH Aachen 1969. VDI Forschungsheft 539, pp 25-48.

/5/ **Dallmeyer, H.** *Stoff- und Wärmeübertragung bei der Kondensation eines Dampfes aus einem Gemisch mit einem nicht kondensierbaren Gas in laminarer und turbulenter Strömungsgrenzschicht.* Diss. an der TH Aachen 1968, VDI Forschungsheft 539, pp 4-24.